

Orientation of He(2¹P) by Electron Impact Excitation and Polarization of the Radiative Decay

D. E. Golden and N. C. Steph

Department of Physics and Astronomy,
University of Oklahoma, Norman, OK 73019, U.S.A.

Abstract

A general description of electron–photon angular correlations is given which relates the quantum-mechanical observables to the structure of the coherently excited state. The wavefunction is expressed in terms of magnetic sublevel amplitudes and state vectors. A semiclassical impact parameter model of orientation is introduced, the experimental considerations are discussed, and experimental results for the orientation and polarization fraction are reviewed.

1. Introduction

The study of the angular correlation between reaction products is a powerful technique that can be used to obtain information about the internal structure of the target. In such a study it is usual to treat the excitation and subsequent decay of the target as independent processes, which implies that the lifetime of the excited state is long enough so that the projectile has left the target before the excited state decays. It should be noted that, if one is dealing with such a problem near a target threshold, such an approximation may not be valid.

If an electron is used as the projectile we have the simplest collision problem that retains the richness afforded by the target structure and allows a straightforward separation of the collision dynamics and the structure. The study of electron–photon angular correlations may be used to obtain all of the quantum-mechanical observables for the problem in terms of excitation amplitudes and relative phases. This knowledge can in turn be used to model the interaction between the electron and target in terms of the parts of the interaction potential which are significant in the different domains of momenta, angular momenta, energy and angle. Going one step further, one could use the experimental data to determine effective electron–atom and molecule scattering potentials, which could be used as models to test the validity of approximations used in *ab initio* calculations.

The theory requires the coherent excitation of the fine and hyperfine levels of the target. Therefore one must choose the target excited state in such a way as to probe a particular aspect of the interaction. For example, if one studies the excitation of the singlet P states of helium, target spin and hyperfine effects can be ignored. If one studies the triplet P states of helium, the effect of target spin must be added to the problem. As problems are probed in greater depth, it may not be adequate to describe the scattering in terms of direct and exchange scattering amplitudes. In such a case the results must be examined in terms of a larger number of scattering

amplitudes in order to account for interactions weaker than Coulombic. For example, the spin-orbit interaction quite generally breaks the scattering planar symmetry so that an observed spin change in a collision may be due to electron exchange (the usual case), or to the spin-orbit coupling of the incident electron or to the spin-orbit coupling in the decaying atom. This means that the total electron spin is not strictly conserved in the collision and additional scattering amplitudes are necessitated by the spin-orbit interaction. These additional amplitudes may be quite small but they will provide an extremely stringent test of theoretical calculations for such processes. The alkali atoms offer the possibility of studying this type of process in one-electron targets where the coupling scheme can be varied from LS to JJ .

In general, as more restrictions are added to the measurement, the problem will be probed in greater depth and additional parameters will be required to characterize the measurement. Energy selectivity may be added to the incident and outgoing electron channels and the photon channel. The spin of the incident and outgoing electrons may be determined and also the initial and final atomic states may be determined at the level of hyperfine structure. In the most general case, partial cross sections for electron-impact excitation of state-to-state hyperfine levels may be obtained.

While a great deal of work has been done to get us to where we are in this subject, there is still a great deal more to do. With this in mind, we turn to the simplest problem: the excitation of the 2^1P state of helium.

2. Excitation Process

The oscillations which were observed in the light intensity in beam-foil experiments (Bashkin and Beauchemin 1966) were first explained by Macek (1969) as being due to interference between hyperfine levels which were excited coherently. This work was extended by Macek and Jaecks (1971) to point out that additional information regarding inelastic scattering could be obtained by studying angular correlations between inelastically scattered electrons and photons from the decay of an excited state, in addition to the measurement of an inelastic cross section. They developed a time-dependent theory of electron impact excitation in which the magnetic substates are excited coherently. For excitation of the 1P states of He, electron spin and hyperfine effects may be neglected and three independent parameters are sufficient to completely determine the excited-state wavefunction. Thus, in this case, one may perform a complete scattering experiment and the most sensitive test of theory for this process.

The wavefunction for the He(2^1P) state may be written

$$\psi(2^1P) = a_0 |10\rangle + a_1 |11\rangle + a_{-1} |1-1\rangle. \quad (1)$$

The incident and scattered electron directions determine the scattering plane, and mirror symmetry in this plane requires that $a_1 = -a_{-1}$. Thus, the three independent parameters are the scattering amplitudes $|a_0|$ and $|a_1|$, and χ , the relative phase between a_0 and a_1 . The total differential cross section is given by

$$\sigma(E, \theta_e) = |a_0|^2 + 2|a_1|^2 = \sigma_0 + 2\sigma_1. \quad (2)$$

The three independent parameters determined by the experiment are σ , λ ($=\sigma_0/\sigma$) and χ .

The first electron-photon angular correlation measurements in helium were done by Eminyan *et al.* (1973) and these measurements have been extended in energy and angular range by many others. Let us consider the electron beam to be incident along the z direction and the helium beam along the y direction as shown in Fig. 1. If we take the xz plane to be the scattering plane and consider photons emitted in the scattering plane, the angular correlation function is given by

$$f(\lambda, \chi, \theta_\gamma) = \lambda \sin^2 \theta_\gamma + (1 - \lambda) \cos^2 \theta_\gamma - \{\lambda(1 - \lambda)\}^{\frac{1}{2}} \cos \chi \cos 2\theta_\gamma. \quad (3)$$

Thus the angular correlation function is periodic in θ_γ and one can determine λ and $|\chi|$ at fixed energy E and scattering angle θ_e by measuring f as a function of θ_γ .

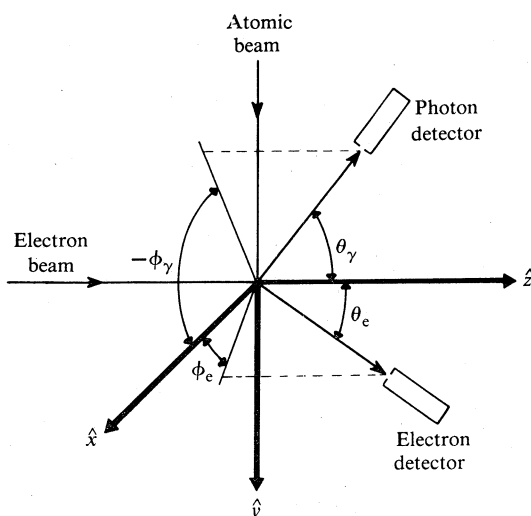


Fig. 1. Schematic diagram of the scattering geometry.

The orientation vector \mathbf{O} and alignment tensor \mathbf{A} were introduced by Fano and Macek (1973) in order to separate the geometrical and dynamical effects. For the 2^1P state, the orientation vector has one non-vanishing component which is proportional to the magnetic dipole moment and given by

$$O_{1-}^{\text{col}} = \frac{1}{2} \langle L_y \rangle = -\{\lambda(1 - \lambda)\}^{\frac{1}{2}} \sin \chi. \quad (4)$$

The alignment tensor is proportional to the electric quadrupole tensor and has three non-vanishing components given by

$$A_0^{\text{col}} = \frac{1}{2} \langle 3L_z^2 - L^2 \rangle = \frac{1}{2} (1 - 3\lambda), \quad (5)$$

$$A_{1+}^{\text{col}} = \frac{1}{2} \langle L_x L_z - L_z L_x \rangle = \{\lambda(1 - \lambda)\}^{\frac{1}{2}} \cos \chi, \quad (6)$$

$$A_{2+}^{\text{col}} = \frac{1}{2} \langle L_x^2 - L_z^2 \rangle = \frac{1}{2} (\lambda - 1), \quad (7)$$

where \mathbf{L} is the total angular momentum and L_i its components. There are only two independent quantities in this set of four. The third independent quantity is the monopole moment which is proportional to σ . It should be noted that in this case all higher multipole moments vanish.

The average value of L_y is twice the orientation and $\langle L_y \rangle$ varies between ± 1 . This reflects the fact that the atom is in a coherent mixture of states without a definite value of m_L . We may then rewrite the wavefunction given in equation (1) as

$$\psi = |a_0| \psi_z + 2^{\frac{1}{2}} |a_1| \exp(ix) \psi_x, \quad (8)$$

where

$$\psi_z = |10\rangle, \quad (9)$$

$$\psi_x = 2^{-\frac{1}{2}}(|11\rangle - |1-1\rangle), \quad (10)$$

and where ψ_z and ψ_x are standing wave p orbitals along the z and x axes respectively.

In this form one can easily see that when λ is 1, the excited state is represented by ψ_z and the orientation is zero, and when λ is 0 the excited state is represented by ψ_x and the orientation is also zero. In fact the orientation is only nonzero when there is a coherent mixture of ψ_x and ψ_z and interference between a_0 and a_1 . The maximum value of the orientation is $\frac{1}{2}$ and the minimum value $-\frac{1}{2}$ but, since experiment only measures $|\chi|$, the sign of the orientation must be specified by theory.

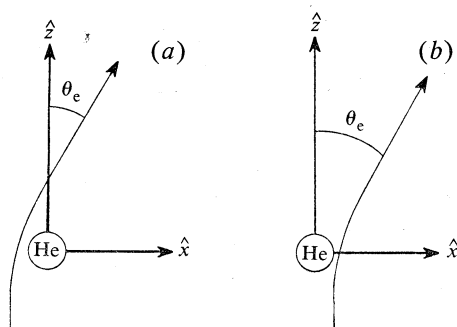


Fig. 2. Semiclassical impact parameter representation of (a) positive orientation for scattering through angle θ_e due to a negative impact parameter and an attractive potential; (b) negative orientation for scattering through angle θ_e due to a positive impact parameter and a repulsive potential.

In order to relate the behaviour of the orientation to the collision process we shall look at the collision semiclassically (Steph and Golden 1980*b*). When an electron is scattered through an angle θ_e the scattering may take place by either of the two paths shown in Fig. 2. In Fig. 2*a* the electron approaches the atom with a negative impact parameter and scatters from an attractive potential to a positive scattering angle. In this case the atom must acquire positive angular momentum perpendicular to the scattering plane, which implies that the orientation is positive. In Fig. 2*b* the electron is incident with a positive impact parameter and must scatter from a repulsive potential to arrive at a positive scattering angle. In this case, in order to conserve angular momentum, the atom must obtain negative angular momentum which implies that the orientation is negative.

When $\theta_e = 0$, the orientation must be zero because there can be no change in angular momentum of the atom perpendicular to the scattering plane. As θ_e increases from zero, the orientation becomes positive because we are dealing with a long-range polarizability potential. It increases towards 0.5 as more and more angular momentum is transferred to the atom perpendicular to the scattering plane. As θ_e continues to increase, the impact parameter decreases and the scattering from the repulsive potential becomes significant. The attractive and repulsive scattering compete and the orien-

tation decreases to zero. Eventually, the repulsive scattering dominates and the orientation decreases towards -0.5 . After the orientation reaches its minimum it must increase to zero, because when $\theta = 180^\circ$ the orientation must again be zero since there can be no change in angular momentum of the atom perpendicular to the scattering plane.

As the energy is increased, the electron spends less time in the long-range field of the attractive potential while the influence of the repulsive potential is not significantly affected by the increased electron velocity. Therefore, as the energy is increased, the maximum of the orientation occurs at smaller and smaller values of θ_e and should not be as large. The zero crossing should decrease in θ_e and the minimum of the orientation should occur at smaller θ_e and become deeper.

It was first pointed out by Standage (1977) that the measurement of λ and σ allows a cascade-free determination of the polarization fraction. The polarization fraction is given by

$$\mathcal{P} = (I_{\parallel} - I_{\perp}) / (I_{\parallel} + I_{\perp}), \quad (11)$$

where I_{\parallel} and I_{\perp} are the light intensities of the emitted radiation polarized parallel and perpendicular to the incident electron beam respectively. The parallel and perpendicular polarizations arise due to the $\Delta m_J = 0$ and $\Delta m_J = \pm 1$ selection rules. The connection between the linear polarizations and the various cross sections was given by Percival and Seaton (1957):

$$\mathcal{P} = (Q_0 - Q_1) / (Q_0 + Q_1), \quad (12)$$

where Q_0 and Q_1 are the partial cross sections for excitation of the degenerate magnetic sublevels $m_J = 0$ and $m_J = \pm 1$ respectively. These partial cross sections can be obtained from measurements of λ and σ as

$$Q_0 = 2\pi \int_0^{\pi} \sigma \lambda \sin \theta_e \, d\theta_e, \quad (13)$$

$$Q_1 = \frac{1}{2}(Q_{\text{tot}} - Q_0), \quad (14)$$

$$Q_{\text{tot}} = 2\pi \int_0^{\pi} \sigma \sin \theta_e \, d\theta_e. \quad (15)$$

3. Experimental Considerations

A schematic diagram of the apparatus used by Steph and Golden (1980a) to measure λ and χ is shown in Fig. 3. Electrons from the electron gun are cross fired with an atomic beam perpendicular to the drawing. The unscattered electrons are collected by a Faraday cup and the scattered electrons are energy analysed by an electron energy analyser (EEA). Photons from the decay are detected by a photon detector. After the EEA has been adjusted to detect electrons which have excited the atomic state of interest, electron pulses are used to start a time-to-amplitude converter (TAC) and delayed photon pulses are used to stop the TAC. The coincidence spectrum is obtained by pulse height analysing the output of the TAC and it is stored in the multichannel analyser. The true starts are also counted and the number of coincidences are normalized to the number of true starts.

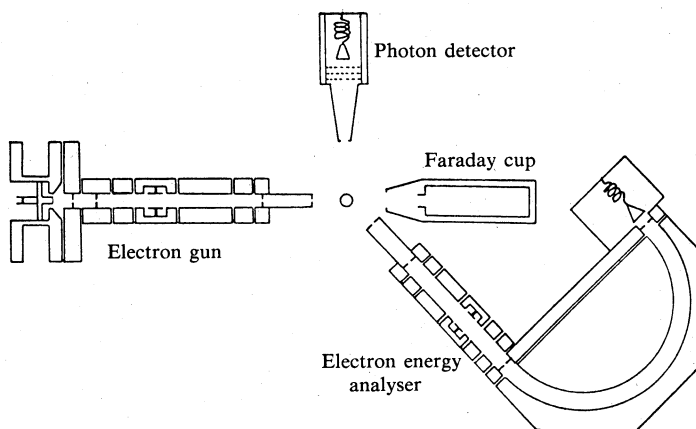


Fig. 3. Schematic diagram of apparatus used by Steph and Golden (1980a) to measure λ and ζ .

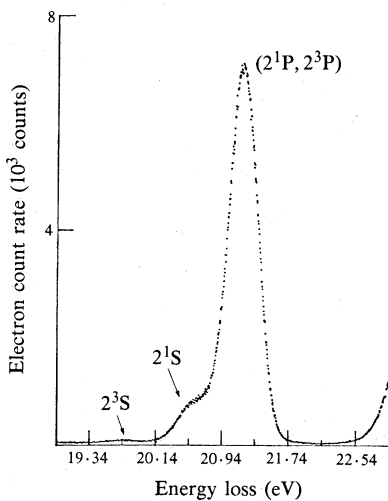


Fig. 4. Energy loss spectrum in helium from about 19 to 23 eV for $\theta_e = 10^\circ$. [Steph and Golden (1980a).]

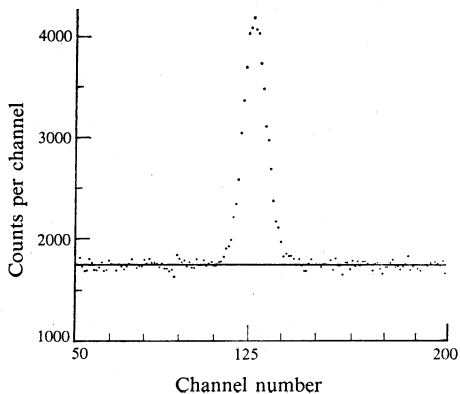


Fig. 5. Coincidence spectrum in helium for excitation of the 2^1P state and its subsequent decay for an incident energy of 80 eV and for $\theta_e = 10^\circ$. [Steph and Golden (1980a).]

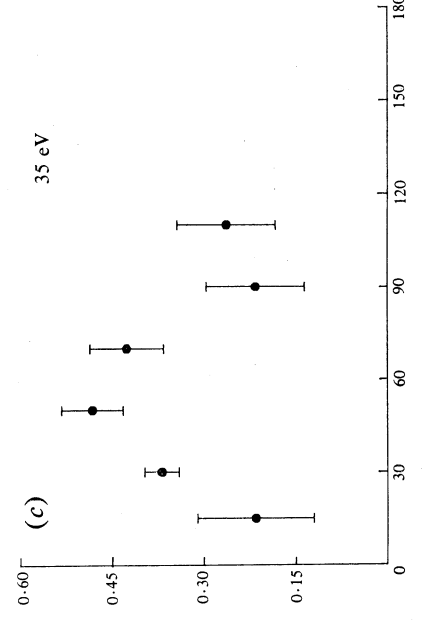
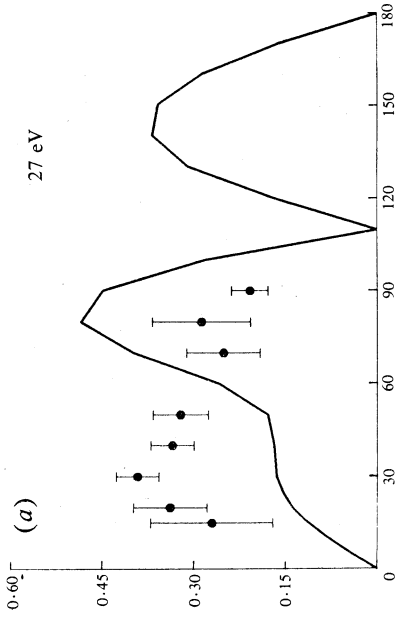
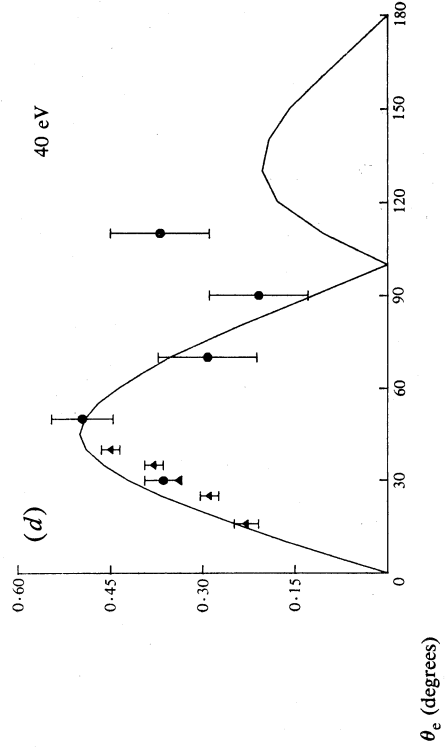
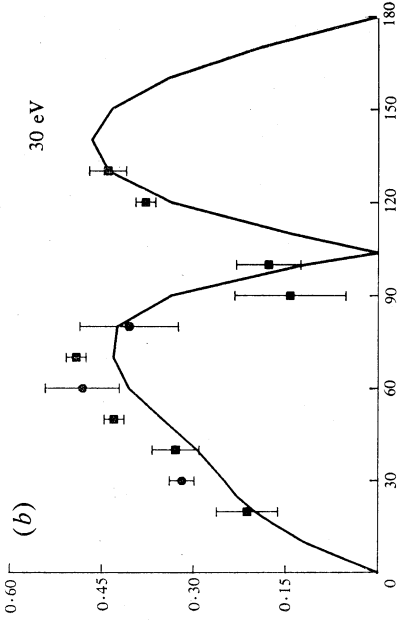
A sample energy loss spectrum for He in the energy range from about 19 to 23 eV is shown in Fig. 4. In the case of excitation of the 2^1P state the energy loss would be fixed at 21.22 eV. A sample coincidence spectrum is shown in Fig. 5. The number of true coincidences is obtained by counting the number in the peak and subtracting the background.

4. Results

The orientation determined from measurements of λ and $|\chi|$ is given in Fig. 6 for the energies 27, 30, 35, 40, 80, 100 and 200 eV. The results of Steph and Golden (1980*b*, 1982*b*) are shown as well as the results of Hollywood *et al.* (1979) and McAdams *et al.* (1980), those of Slevin *et al.* (1980) and those of Emynyan *et al.* (1973, 1974). The *R*-matrix calculations of Fon *et al.* (1979) are shown by the thick curves and the distorted wave calculations of Madison (1979) are shown by the thin curves. The results are by and large in better agreement with the calculation of Madison, and the different experimental data are in good agreement, with the exception of the large-angle results at 80 eV (Fig. 6*e*). The variation of $|O_1^-|$ with increasing energy is in agreement with the semiclassical model described above. This can be most readily seen in Fig. 7 where the calculations of Madison (1979) at 80, 100, 150 and 200 eV are presented on a common plot.

The agreement with the semiclassical model continues as the energy is decreased from 80 to 30 eV (Figs 6*e-b*). The width of the small-angle maximum increases as both the maxima and the zero crossing move to larger angles. This behaviour would be expected as the energy decreases and, for a given impact parameter, the electron spends more time in the field of the long-range potential and scatters to larger angles. At 27 eV (Fig. 6*a*) the behaviour of $|O_1^-|$ changes. The positive maximum occurs at a much smaller angle, and there is evidence of a second maximum at about 80° , before the zero crossing. As the energy approaches threshold, the broad resonances near the excitation threshold significantly affect the scattering and a semiclassical model cannot be adequate. The effect of these resonances has been seen in measurements of the polarization fraction at energies below 40 eV. There is a marked and unexpected decrease in polarization as threshold is approached, followed by a sharp increase to $\mathcal{P} = 1$ at threshold. Since direct measurements of \mathcal{P} cannot eliminate cascade contributions, the results extracted from correlation experiments are particularly interesting.

In Fig. 8 the cascade-free results of Steph and Golden (1982*a*) are compared with the previous direct measurements of Mumma *et al.* (1974) for the sum of the $n^1\text{P} \rightarrow 1^1\text{S}$ transitions and the previous cascade-free results of Standage (1977). The difference between the result of Standage (1977) and that of Steph and Golden (1982*a*) at 60 eV reflects the improved angular range of the data. One would expect the cascade-free results to be larger than the results of Mumma *et al.* (1974) since the effect of cascade contributions is to populate the magnetic sublevels more uniformly. The present results indicate that the fall in \mathcal{P} with decreasing E to zero near threshold and its subsequent rise to 1 at threshold must be much sharper than previously observed. This would be expected if the decrease in polarization is due to ^2P and ^2D resonances below the threshold. In such a case, the $L = 1$ and 2 partial waves would make large contributions to the scattering, and the excitation of the $m_j = 1$ state would probably be near threshold. Close coupling calculations using such ideas



$|O_{1-}|$

θ_e (degrees)

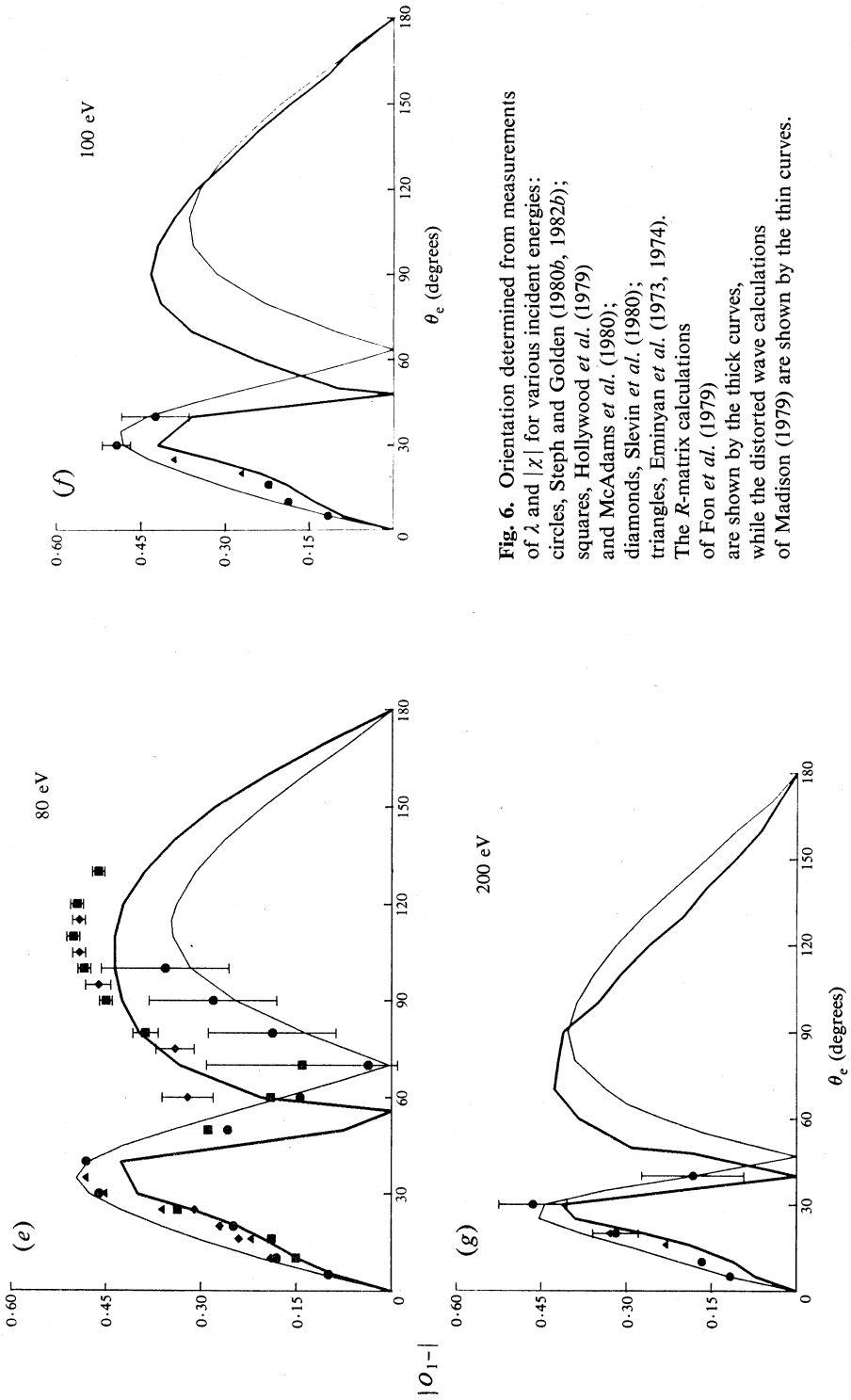


Fig. 6. Orientation determined from measurements of λ and $|\chi|$ for various incident energies: circles, Steph and Golden (1980b, 1982b); squares, Hollywood *et al.* (1979) and McAdams *et al.* (1980); diamonds, Slevin *et al.* (1980); triangles, Emynan *et al.* (1973, 1974). The R -matrix calculations of Fon *et al.* (1979) are shown by the thick curves, while the distorted wave calculations of Madison (1979) are shown by the thin curves.

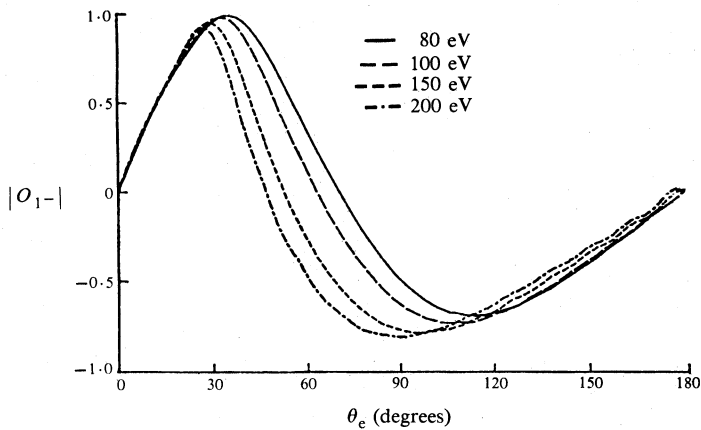


Fig. 7. Orientation as calculated by Madison (1979) for incident energies of 80, 100, 150 and 200 eV.

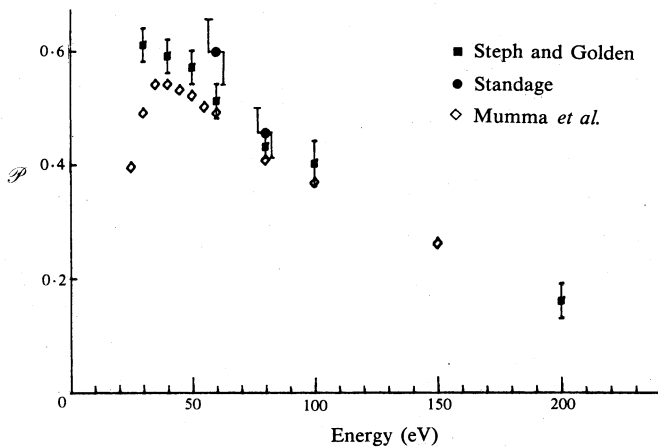


Fig. 8. Polarization fraction for the $2^1\text{P} \rightarrow 1^1\text{S}$ transition in He from Steph and Golden (1982a) and Standage (1977). The results are compared with those for $\sum n^1\text{P} \rightarrow 1^1\text{S}$ by Mumma *et al.* (1974).

were carried out by Burke *et al.* (1969). These calculations showed that \mathcal{P} fell from 1 at threshold to 0.6 at 22.5 eV, but no detailed calculations have been carried out beyond 22.5 eV. The polarization fraction of an $n^1\text{P}$ state seems to increase slightly with n . This might explain why Mumma *et al.* (1974), who observed $\sum n^1\text{P} \rightarrow 1^1\text{S}$ transitions, found values of \mathcal{P} consistently larger than those of Heddle and Lucas (1963), who observed only the $3^1\text{P} \rightarrow 2^1\text{S}$ transition. The increase of \mathcal{P} with principal quantum number is predicted by the Born approximation.

Acknowledgment

This work was supported by the NSF and AFOSR.

References

- Bashkin, S., and Beauchemin, G. (1966). *Can. J. Phys.* **44**, 1603.
- Burke, P. G., Cooper, J. W., and Ormonde, S. (1969). *Phys. Rev.* **183**, 245.
- Eminyan, M., MacAdams, K. B., Slevin, J., and Kleinpoppen, H. (1973). *Phys. Rev. Lett.* **31**, 576.
- Eminyan, M., MacAdams, K. B., Slevin, J., and Kleinpoppen, H. (1974). *J. Phys.* B **7**, 1519.
- Fano, U., and Macek, J. H. (1973). *Rev. Mod. Phys.* **45**, 553.
- Fon, W. C., Berrington, K. A., and Kingston, A. E. (1979). *J. Phys.* B **12**, L171.
- Heddle, D. W. O., and Lucas, C. B. (1963). *Phil. Trans. R. Soc. London A* **271**, 129.
- Hollywood, M. T., Crowe, A., and Williams, J. F. (1979). *J. Phys.* B **12**, 819.
- McAdams, R., Hollywood, M. T., Crowe, A., and Williams, J. F. (1980). *J. Phys.* B **13**, 3691.
- Macek, J. (1969). *Phys. Rev. Lett.* **23**, 1.
- Macek, J., and Jaecks, D. H. (1971). *Phys. Rev. A* **4**, 2288.
- Madison, D. H. (1979). *J. Phys.* B **12**, 3399.
- Mumma, M. J., Misakian, M., Jackson, W. M., and Faris, J. L. (1974). *Phys. Rev. A* **9**, 203.
- Percival, I. C., and Seaton, M. J. (1957). *Proc. Cambridge Philos. Soc.* **53**, 654.
- Slevin, J., Porter, H. Q., Eminyan, M., DeFrance, A., and Vassilev, G. (1980). *J. Phys.* B **13**, 3009.
- Standage, M. C. (1977). *J. Phys.* B **10**, 2789.
- Steph, N. C., and Golden, D. E. (1980a). *Phys. Rev. A* **21**, 759.
- Steph, N. C., and Golden, D. E. (1980b). *Phys. Rev. A* **21**, 1848.
- Steph, N. C., and Golden, D. E. (1982a). *Phys. Rev. A* **26**, 148.
- Steph, N. C., and Golden, D. E. (1982b). Low-energy measurements of electron-photon angular correlation in electron impact excitation of the 2^1P state of helium. *Phys. Rev. A* (to be published).

Manuscript received 29 April, accepted 9 September 1982

